

Generative Adversarial Talking Head: Bringing Portraits to Life with a Weakly Supervised Neural Network

Hai X. Pham, Yuting Wang & Vladimir Pavlovic

Department of Computer Science, Rutgers University
{hxp1,yw632,vladimir}@cs.rutgers.edu

Abstract. This paper presents *Generative Adversarial Talking Head (GATH)*, a novel deep generative neural network that enables fully automatic facial expression synthesis of an arbitrary portrait with continuous action unit (AU) coefficients. Specifically, our model directly manipulates image pixels to make the unseen subject in the still photo express various emotions controlled by values of facial AU coefficients, while maintaining her personal characteristics, such as facial geometry, skin color and hair style, as well as the original surrounding background. In contrast to prior work, GATH is purely data-driven and it requires neither a statistical face model nor image processing tricks to enact facial deformations. Additionally, our model is trained from unpaired data, where the input image, with its auxiliary identity label taken from abundance of still photos in the wild, and the target frame are from different persons. In order to effectively learn such model, we propose a novel weakly supervised adversarial learning framework that consists of a generator, a discriminator, a classifier and an action unit estimator. Our work gives rise to *template-and-target-free expression editing*, where still faces can be effortlessly animated with arbitrary AU coefficients provided by the user.

Keywords: generative adversarial learning, automatic facial animation, still portrait, action unit

1 Introduction

Human faces convey a large range of semantic meaning through facial expressions, which reflect both actions e.g. talking, eye-blinking, and emotional states such as happy (smiling), sad (frowning) or surprised (raising eyebrows). Over the years, much research has been dedicated to the task of facial expression editing, in order to transfer the semantic expression from a target to a source face, with impressive results [1,2,3,4,5]. In general, these state-of-the-art techniques assume that a pair of source-target images is available, and there exists a pair of matching 2D or 3D facial meshes in both images for texture warping and rendering. Additionally, recent work by Thies et al. [2] and Cao et al. [6] require a set of source images in order to learn a statistical representation, that can be used to create a source instance at runtime. The above requirement limits the application of these techniques to certain settings, where source data is abundant. In [1,5,7], the authors propose to directly transfer expressions from the target image



(a) source and target are of the same subject (b) source and target are from different persons

Fig. 1: Some samples generated by our proposed GATH model. Each triplet consists of the source, the target and the synthesis. Note that our model only knows the source image and a vector of action unit coefficients that resemble the target. Could the reader tell apart which image is the source, target and synthesis? Hint: start with (b) first.

to the source face, forgoing the need of prior statistics of the source subject. However, there are situations in which the target face to drive facial deformation of the source does not exist, instead, facial expression can be inferred from other input modalities, such as speech [8,9,10], or explicitly specified by user as vector of facial action unit (AU) intensities [11].

In this work, we are interested in mid-level facial expression manipulation by directly animating a human portrait given only AU coefficients, thereby enabling a whole new level of flexibility to the facial expression editing task. Particularly, our proposed GATH model is able to modify a frontal face portrait of arbitrary identity and expression at pixel level, hallucinating a novel facial image whose expressiveness mimics that of a real face that has similar AU attributes. In other words, our model learns to extract identity features to preserve individual characteristic of the portrait, facial enactment to animate the portrait according to values of AU coefficients and texture mapping, all in an end-to-end deep neural network.

Learning identity features requires a large number of training images from thousands of subjects, which are readily available in various public datasets. On the other hand, the amount of publicly available emotional videos such as [12], from which we could collect a wide range of AU coefficients, is rather limited. A deep net trained on such a small number of subjects would not generalize well to unseen identity. To address this shortcoming, we propose to train the deep net with separate source and target sets, i.e. the animated facial image of subject A in the source set does not have an exact matching target image, but there exists an image of subject B in the target set that has similar expression to the synthesized image of A, and their expressiveness similarity is measured by an auxiliary function. Inspired by recent advances in image synthesis with adversarial learning [13,14], we jointly train the deep face generator with a discriminator in a minimax game, in which the generator gradually improves the quality of its synthesis to try to fool the discriminator in believing that its output is from the real facial image distribution. Furthermore, taking advantage of the availability of subject class labels in the source set, we jointly train a classifier to recognize the subject label

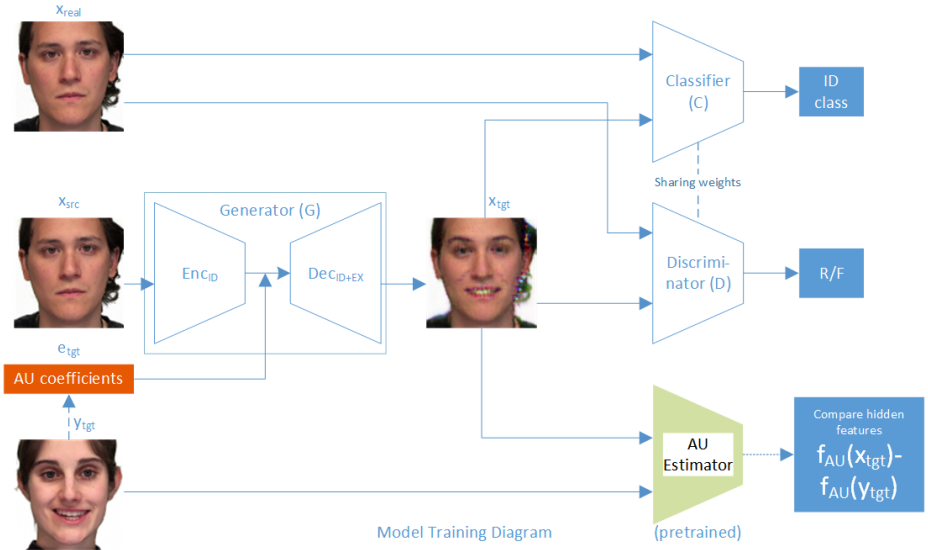


Fig. 2: The proposed GATH learning framework. Except for the AU Estimator that is pretrained, other networks including the generator, the discriminator and the classifier are jointly trained. The discriminator and the classifier share hidden layer weights. The generator only knows AU coefficients e_{tgt} extracted from target frame y_{tgt} . The generator G learns to produce output x_{tgt} from input image x_{src} , such that the synthesized face has similar facial expression as the target frame y_{tgt} . x and y are different subjects.

of the generated output, therefore encouraging the generator to correctly learn identity features, and producing better synthesis of the input subject.

Our main contributions are as follows:

- Generative Adversarial Talking Head, a deep model that can generate realistic expressive facial animation from arbitrary portraits and AU coefficients. The model is effectively trained in an adversarial learning framework including a generator, a discriminator and a classifier, where the discriminator and the classifier supervise the quality of synthesized images, while the generator learns facial deformations from separate source and target image sets, and is able to disentangle latent identity and expression code from the source image.
- An action unit estimator (AUE) network, whose hidden features are used as an expressiveness similarity measure between the synthetic output and its unpaired target facial image in order to guide the generator to synthesize images with correct expression.
- Extensive evaluations and applications to demonstrate the effectiveness and flexibility of our proposed model in animating various human portraits from video-driven and user-defined AU coefficients.

2 Related Work

”Talking head”. As the title suggests, our work is inspired by the line of research in synthesizing talking faces from speech [10,15,16,8,17,18,19], in which the face is animated to mimic the continuous time-varying context (i.e. talking) and affective states carried in the speech. In recent years, deep neural networks (DNN) have been successfully applied to speech synthesis [20,21] and facial animation [22,23,10] with superior performance. Taylor et al. [19] propose a system using DNN to estimate active appearance model (AAM) coefficients from phonemes. Suwajanakorn et al. [18] use long short-term memory (LSTM) recurrent net to predict 2D lip landmarks from input acoustic features for lip-syncing. Fan et al. [10] estimate AAM coefficients of the mouth area, whose texture is grafted onto an actual image to produce a photo-realistic talking head. Pham et al. [8] map acoustic features to action unit coefficients with an LSTM network to drive a 3D blendshape face model. Such model can be integrated into our GATH framework to drive facial expression synthesis from speech.

Generative Adversarial Nets (GAN). Proposed by Goodfellow et al. [13], GAN learns the generative model in a minimax game, in which the generator and discriminator gradually improve themselves.

$$\min_G \max_D E_{x \sim p_{data}(x)} [\log D(x)] + E_{z \sim p(z)} [\log (1 - D(G(z)))]. \quad (1)$$

Eventually the generator learns to create realistic data able to fool the discriminator. GAN has been widely used in image synthesis with various successes [24,25,14,26,27,28]. Moreover, recent works also introduce additional constraints for topic-driven synthesis [29], or use class labels in semi-supervised GAN training [30,31,32,33]. In our approach, a classifier is jointly trained with the discriminator to predict synthesized images into C classes. Consequently, not only the generator learns to generate realistic images, but the synthesis also preserves the identity presented in the source image.

Facial image editing. Facial editing techniques in literature are mostly model-based, using a 3DMM [34,35], and follow a common approach, in which a 3DMM is fitted to both source and target images, and the target expression is transferred to the source frame by manipulating the model coefficients to calculate a new 3D facial shape, followed by texture remapping [36,2,4,3,37,38]. Averbuch-Elor et al. [1] only use 2D face alignment with clever texture warping and detail transfer [39]. Instead of using graphics-based texture warping, Orszewski et al. [5] utilize supervised GAN to synthesize a new albedo in the UV texture space, given matching source and target images. In a different approach, Liu et al. [40] uses conditional GAN to synthesize expression coefficients of a 3DMM given discrete AU labels, followed by standard shape calculation and texture remapping. Based on variational autoencoder (VAE) [41], Yet et al. [7] train an expression flow VAE from matching source-target pairs, and edit the latent code to manipulate facial expression. *Deepfakes* [42], which has gone viral on the internet recently, uses coupled autoencoders and texture mapping to be able to swap identities of two actors. In contrast to model-based approaches, our model directly generates the facial image from source portrait and target AU coefficients without using a statistical face model or a target video for transferring, forgoing manual texture warping and blending as these tasks are automatically carried out by the deep net. Different

from recent GAN-based synthesis models, our method trains the generator from totally unmatched source-target pairs.

Representation disentangling. It is still an open question of how to design proper objectives that can effectively learn good latent representation from data. Kulkarni et al. [43], Yang et al. [44] propose models that can explicitly separate different codes (object type, pose, lighting) from input images. Those codes can be manipulated to generate a different looking image, e.g. by changing the pose code. Peng et al. [45] propose a recurrent encoder-decoder network for face alignment, that also learns to separate identity and expression codes through a combination of auxiliary networks and objectives. Tran et al. [32] employ semi-supervised GAN to learn disentangled face identity/pose for face frontalization. GATH is similar in spirit to [32], in which the encoder subnetwork of the generator learns the latent identity code independently from the arbitrary expression in the source image, and the decoder takes in the combined identity and AU code to generate an animated image from the source portrait.

3 Proposed Model

3.1 Problem Formulation

We first denote the following notations that will be used throughout the paper: G = generator; $f_{G.en}$ = encoder subnetwork of G ; $f_{G.de}$: decoder subnetwork of G ; D = discriminator; \mathcal{C} = classifier; \mathcal{E} = AU Estimator; f_{au} = a function that maps image to a latent facial expression space; x_{src} = source portrait to be transformed; x_{tgt} = image synthesized by the generator; x_{re} = real image used to train D and \mathcal{C} ; c = the class label associated with x_{re} ; y_{tgt} = target image; e_{tgt} = continuous AU coefficient vector corresponding to y_{tgt} . x_{src} and x_{re} are sampled from the same training source set, and are not necessarily the same. y_{tgt} is sampled from the training target set. e_{tgt} is a 46-D vector in which each component varies freely in $[0,1]$, following the convention of the FaceWarehouse database [46].

Our general GATH framework is illustrated in Figure 2. The generator G synthesizes x_{tgt} from the input x_{src} given AU coefficients e_{tgt} : $x_{tgt} = G(x_{src}, e_{tgt}) = f_{G.de}(f_{G.en}(x_{src}), e_{tgt})$. Since x_{src} may contain arbitrary expression, the generator specifically disentangles the latent identity code from expression features in the source image with the encoder, effectively making the transformation of the source face independent of the expression manifested in the input image.

Unlike previous work [5,7], our source and target sets are disjoint¹. In other words, an exact correspondence y_{tgt}^0 of x_{tgt} does not exist, hence we are unable to use the conventional pixel-wise reconstruction loss to learn facial deformation. However, there exists a frame y_{tgt} that shares similar values of AU intensities to x_{tgt} . One might naively minimize the difference $\|x_{tgt} - y_{tgt}\|$, but using this loss has major drawbacks: Firstly, there is not necessarily pixel-wise correspondence between x_{tgt} and y_{tgt} , hence a local facial deformation at a specific coordinate in the target does not mean that the same visual change would also happen at the exact same coordinate in the source. Secondly,

¹ In training, we actually mix a small amount of image samples of subjects in the target set into the source set, which accounts for 2.7% of its size, to increase its diversity.

directly minimizing the difference between the source and the target frame would make the model learn to hallucinate the identity of the target into the source, which violates the identity preserving aspect of our model. Furthermore, what we want to compare is the expressiveness similarity of the source and target, not their entire appearances. Inspired by recent work in artistic style transfer [47], we wish to compare the source and target in a latent expressiveness space with a projecting function f_{au} . Thus, we propose to train a deep Action Unit Estimator network, and measure the similarity of source and target in the hidden feature space of AUE.

One core objective of our work is to learn a generator G that can generate realistic looking face synthesis indistinguishable from a real image, especially in our case where the exact corresponding target does not exist. To this end, we integrate the adversarial loss proposed by Goodfellow et al. [13] into our framework, by jointly training a discriminator D that can tell the difference between real and fake images, that eventually guides G to generate "fine enough" samples via a minimax game.

A straightforward approach to learn identity disentanglement is to minimize the intra-subject reconstruction loss $\|x_{tgt} - x_{src}\|$, as they are largely similar except sparse local deformation parts. However, we can utilize the available auxiliary class labels of the source set to provide additional feedback to make the generator learn the disentanglement more effectively. We propose to jointly train a classifier \mathcal{C} that share all hidden layer weights with the discriminator. The advantages of this approach are two-fold. First, jointly learning the classifier \mathcal{C} and discriminator D helps discover relevant facial hidden features better, and D can tell apart the real image from the fake more easily. In return, these players provide stronger feedback to the generator, encouraging G to generate finer synthesis and better preserve the identity of the source.

3.2 Action Unit Estimator

We propose a CNN model \mathcal{E} based on VGG-9 architecture [48] to predict AU coefficients from a facial image: $\mathcal{E} : x \rightarrow e$. The network architecture is shown in Figure 3c. \mathcal{E} is learned by minimizing the squared loss:

$$\min_{\mathcal{E}} \|e_{gt} - \mathcal{E}(x)\|_2^2, \quad (2)$$

where e_{gt} is a ground truth AU vector. In essence, AUE learns hidden features tailored to facial expression and independent of identity, as well as invariant to position and scale of the face in the image. We take the last convolutional layer of AUE as the latent space mapping function f_{au} to measure the expressiveness similarity of images. First, this layer retains high-level features with rich details to represent the facial expression. Furthermore, the convolutional layer still preserves the spatial 2D structure layout, hence it can pinpoint where in the source image that the local deformation should happen.

3.3 GATH Learning

The models in our framework are jointly trained by optimizing the following composite loss:

$$\mathcal{L}_{au} + \lambda_{rec}\mathcal{L}_{rec} + \lambda_{adv}\mathcal{L}_{adv} + \lambda_{cls}\mathcal{L}_{cls} + \lambda_{tv}\mathcal{L}_{tv}. \quad (3)$$

The first term is the AU loss, to make G learn to expressively transform the source image to manifest the target emotion:

$$\mathcal{L}_{au} = \min_G \|f_{au}(y_{tgt}) - f_{au}(G(x_{src}, e_{tgt}))\|_2^2. \quad (4)$$

The intra-subject reconstruction loss, \mathcal{L}_{rec} , minimizes the pixel-wise difference between the source and the synthesized image, to preserve the subject identity as well as the background:

$$\mathcal{L}_{rec} = \min_G \|x_{src} - G(x_{src}, e_{tgt})\|_1. \quad (5)$$

The third term is the adversarial loss. In this work, we replace the vanilla Jensen-Shannon divergence GAN loss in (1) with the least square loss proposed in CycleGAN [49], as we found that this objective makes optimization more stable.

$$\mathcal{L}_{adv} = \max_G \min_D (1 - D(x_{re}))^2 + (D(G(x_{src}, e_{tgt})))^2. \quad (6)$$

The classifier loss, \mathcal{L}_{cls} , consists of two cross-entropy loss terms. Minimizing the first term updates the weights of the classifier, while the second term updates the weights of G . Intuitively, the classifier updates its parameters from real image samples x_{re} , and provides feedback to the generator, such that G learns to generate better samples to lower the classification loss, and consequently preserve the source identity better.

$$\mathcal{L}_{cls} = \min_C - \sum_i c_i \log \mathcal{C}_i(x_{re}) + \min_G - \sum_i c_i \log \mathcal{C}_i(G(x_{src}, e_{tgt})). \quad (7)$$

The last term is total variation loss to maintain spatial smoothness:

$$\mathcal{L}_{tv} = \sum_{i,j} \left(x_{tgt}^{i,j+1} - x_{tgt}^{i,j} \right)^2 + \left(x_{tgt}^{i+1,j} - x_{tgt}^{i,j} \right)^2. \quad (8)$$

In the adversarial learning framework, the generator and discriminator are alternatively and iteratively updated. Essentially, in GATH, the joint discriminator-classifier network is updated by minimizing this loss:

$$\begin{aligned} \min_{D,C} \lambda_{adv} \left[(1 - D(x_{re}))^2 + (D(G(x_{src}, e_{tgt})))^2 \right] \\ - \lambda_{cls} \sum_i c_i \log \mathcal{C}_i(x_{re}), \end{aligned} \quad (9)$$

whereas minimizing the following composite loss updates the generator:

$$\begin{aligned} \min_G \mathcal{L}_{au} + \lambda_{rec} \mathcal{L}_{rec} + \lambda_{tv} \mathcal{L}_{tv} - \lambda_{adv} (D(G(x_{src}, e_{tgt})))^2 \\ - \lambda_{cls} \sum_i c_i \log \mathcal{C}_i(G(x_{src}, e_{tgt})). \end{aligned} \quad (10)$$

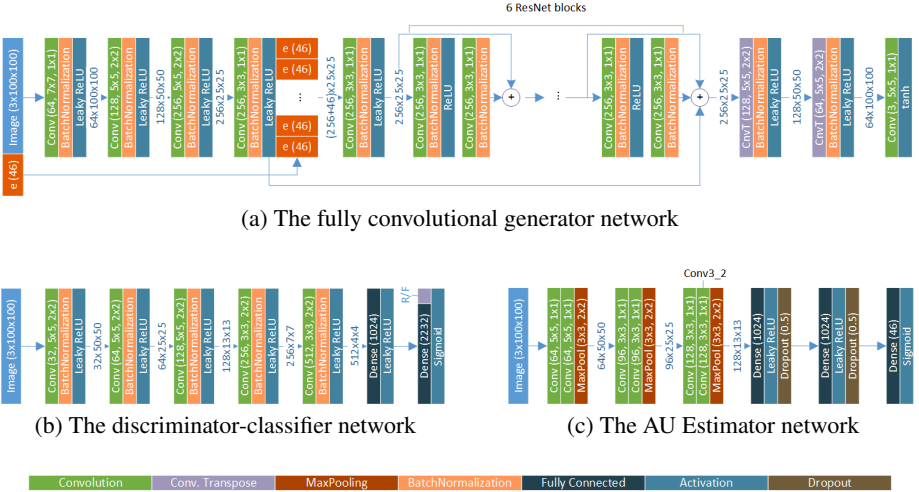


Fig. 3: (*best viewed in color*) Architectures of deep neural networks in our GATH framework. The last convolutional layer of the AUE, 'conv3_2', is used to extract expressive hidden features to calculate \mathcal{L}_{AU} .

4 Implementation Details

4.1 Network Architecture

Architectures of three networks in our GATH framework are illustrated in Figure 3. These networks are designed such that all of them can reside in the GPU memory of a Tesla K40 at the same time.

The input to each network is a standard 100x100px RGB image, with pixel values normalized to $[-1, 1]$. The generator G includes two subnetworks: encoder and decoder. The encoder consists of four blocks, each one starts with a convolutional layer, followed by a batch normalization layer and Leaky ReLU activation with slope factor of 0.1. The AU vector is concatenated to the output of the forth block by spatially 2D broadcasting. The decoder starts with a convolutional block, followed by six ResNet [50] blocks, two convolutional transpose blocks and a final convolutional output layer. Particularly, there is a residual connection from the output of the encoder to the end of the bottle neck to help G learn the identity code more effectively.

Figure 3b shows the weight sharing discriminator-classifier network. D and C share all hidden layer parameters, but have separate output layers.

4.2 Training and Post-processing

Training. We organize the source set as a combination of the following still photo datasets: Cross-age Celebrity dataset (CACD) [51], FaceWareHouse [46], GTAV [52], consisting of 2,168 identities. We also mix in a small set of frames from 20 actors in RAVDESS [12] and 40 actors in VIDTIMIT [53] dataset, making a total of 2,228 identities in the source set.

The target set consists of a large number of frames extracted from RAVDESS and VIDTIMIT, two popular audiovisual datasets, in which actors display a wide range of facial actions and emotions. We extract AU coefficients from these two datasets using a performance-driven 3D face tracker [54,55]. The AUE is trained on the target set.

Furthermore, since these datasets include many face images at large pose, we use the face frontalization technique proposed by Hassner et al. [56] to roughly convert original images into portraits in both source and target sets and crop them to 100x100px. The alignment is not perfect, however, our AUE is invariant to translation and scale, hence our generator can learn facial deformation reliably.

The models in our GATH framework, G , D and \mathcal{C} , are trained end-to-end with the ADAM minibatch optimizer [57]. We set minibatch size = 64, initial learning rate = $1e-4$ and momentum = 0.9. Other hyperparameters in (3) are empirically chosen as follows: $\lambda_{rec} = \lambda_{tv} = 1.0$, $\lambda_{adv} = \lambda_{cls} = 0.05$. The whole framework² is implemented in Python based on the deep learning toolkit CNTK³.

Post-processing. A side effect of using the composite loss in (3) to train our weakly supervised model and pixel scaling to and from the [-1,1] range is that the synthesis loses the dynamic range of the original input. In order to partially restore the original contrast, we apply the adaptive histogram equalization algorithm CLAHE [58] to synthesized images. Parts of evaluation where CLAHE is applied will be clearly indicated. Furthermore, for visualization purpose, we clear the noise in the output with non-local means denoising [59], followed by unsharp masking. Figure 4b demonstrates the visual effects of these two enhancements on the syntheses.

5 Evaluation

Due to the lack of a publicly available implementation of the face editing methods mentioned in Section 2, we simplify our GATH framework to create two baselines. **GATH-DC** (GATH *minus* DC): GATH without the joint discriminator-classifier network; **GATH-C**: GATH without the classifier.

For quantitative evaluation, we record facial expression synthesizing performance on a hold out test set of four actors from RAVDESS and three actors in VIDTIMIT, which are not included in training. Specifically, we choose two source frames from each actor. In one frame, the actor displays neutral (or close to neutral) expression. In the other one, the actor shows at least one expression (mouth opening). Each source image is paired with all video sequences (94 in total), resulting in 188 intra-class (same subject) pairs and 1032 inter-class pairs, where the source actor is different from the target actor.

We quantify the synthesis performance of our model with a set of metrics: for intra-class experiments, we measure the pixel-wise Mean Absolute Error (MAE) and Root Mean Square Error (RMSE), as well as the AU error (RMSE of intensity values), with respect to ground truth frame. We use the OpenFace toolkit [60] to extract intensities of 17 AUs (which are different from our set of 46 AUs), each value varies within the range

² code will be published soon, stay tuned!

³ <https://github.com/microsoft/cntk>

of [0,5] (note that our input AU coefficients vary in [0,1]). For inter-class experiments, we only measure the AU error.

We also provide qualitative experiments on a random set of actors from the two popular face datasets: CelebA [61] and Labeled Face in the Wild (LFW) [62].

Lastly, we present an application of *template-and-target-free expression editing*, where user-defined AU coefficients are used to transform arbitrary sources. Mainly within the scope of this paper, we perform expression suppression (i.e. neutralization). However, our model is flexible enough to transform a source facial image with any arbitrary AU values.

5.1 Intra-class Synthesis Evaluation

Table 1 shows pixel-wise MAE and RMSE when comparing the synthesized output with the ground truth image of the same subject (i.e. x_{tgt} and y_{tgt} are of the same person, manifesting the same expression and they should look the very similar). The errors are organized by dataset, and gathered from four different settings: whether taking the background error into account or not (by using a mask to localize the face region), and whether using CLAHE to increase the contrast of the outputs. It is observed that training only the generator, without feedback from the discriminator and classifier, actually makes the model produce better pixel-wise color reconstruction without using histogram equalization, although the difference in error is rather small. After apply CLAHE, the generated outputs of GATH have smallest errors. It is also observed from Table 1 that the reconstructed background pixels actually incur higher error than the face region. In addition, the error heat map in Figure 4 indicates that errors on the face region are almost uniform, indicating a constant shift in the color space.

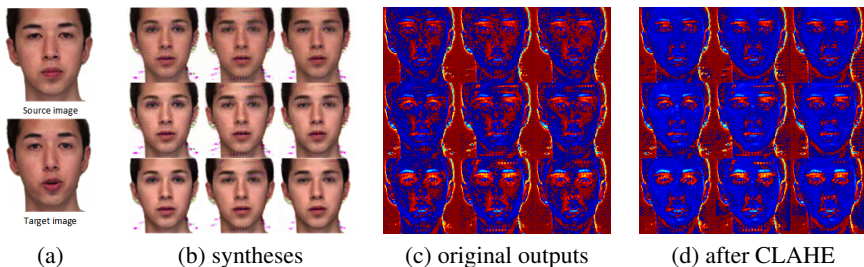


Fig. 4: (a) Source and target images of the same tester. (b) From left to right: syntheses created by two baselines and GATH; top to bottom: raw outputs, histogram-equalized (CLAHE) outputs and sharpened outputs, respectively. (c,d) The pixel-wise error heat maps of one sample in two cases: the raw output and CLAHE-applied output. In each figure, from left to right: output error of GATH-DC, GATH-C and GATH, respectively; from top to bottom: error heat maps on three channels B, G and R, respectively.

However, color reproduction is only one criterion to measure the quality of expression synthesis. Our main objective in this paper is to synthesize animation driven by AU

Table 1: Pixel-wise MAE and RMSE of intra-class synthesis.

	MAE			RMSE		
	RAVDESS	VIDTIMIT	All	RAVDESS	VIDTIMIT	All
full image, without CLAHE						
GATH-DC	141.53	112.78	127.16	182.31	162.47	172.68
GATH-C	144.8	119.13	131.97	184.66	167.34	176.21
GATH	146.46	118.53	132.5	185.8	167.02	176.66
full image, with CLAHE						
GATH-DC	94.49	58.66	76.58	138.62	94.26	118.53
GATH-C	92.31	59.35	75.83	136.86	95.23	117.89
GATH	91.65	59.66	75.66	136.21	95.89	117.79
mask, without CLAHE						
GATH-DC	128.48	122.36	125.42	174	170.94	172.47
GATH-C	134.78	128.53	131.66	178.44	175.48	176.97
GATH	136.14	130.16	133.15	179.48	176.78	178.13
mask, with CLAHE						
GATH-DC	56.47	55.42	55.94	93.42	85.49	89.54
GATH-C	57.37	55.28	56.32	94.84	85.26	90.18
GATH	55.88	54.97	55.43	92.63	84.47	88.64

Table 2: RMSE of Action Unit Intensity in intra-class synthesis.

	RAVDESS	VIDTIMIT	All
GATH-DC	0.592	0.35	0.486
GATH-C	0.591	0.336	0.481
GATH	0.585	0.334	0.477

coefficients. The AU estimation errors with respect to the ground truth frame are shown in Table 2. It proves that the output of GATH has higher fidelity than the two baselines, as better images will help OpenFace estimate AU intensities more accurately. It is also unsurprising that GATH-C, trained jointly with a discriminator, performs better than GATH-DC. These results prove the benefit of our proposed GATH model in synthesizing facial expressions.

Figures 5, 6 demonstrate the synthetic results of GATH. The generated texture has been enhanced visually with the aforementioned post-processing procedure. Notice that in Figure 5b,c,d, it is shown that our model is able to hallucinate eye-blinking motions.

5.2 Inter-class Synthesis Evaluation

In this evaluation, we compare the AU estimation scores returned by OpenFace on the ground truth of a subject, and scores on the corresponding syntheses. The results are shown in Table 3. Once again, the full GATH model outperforms the two baselines.

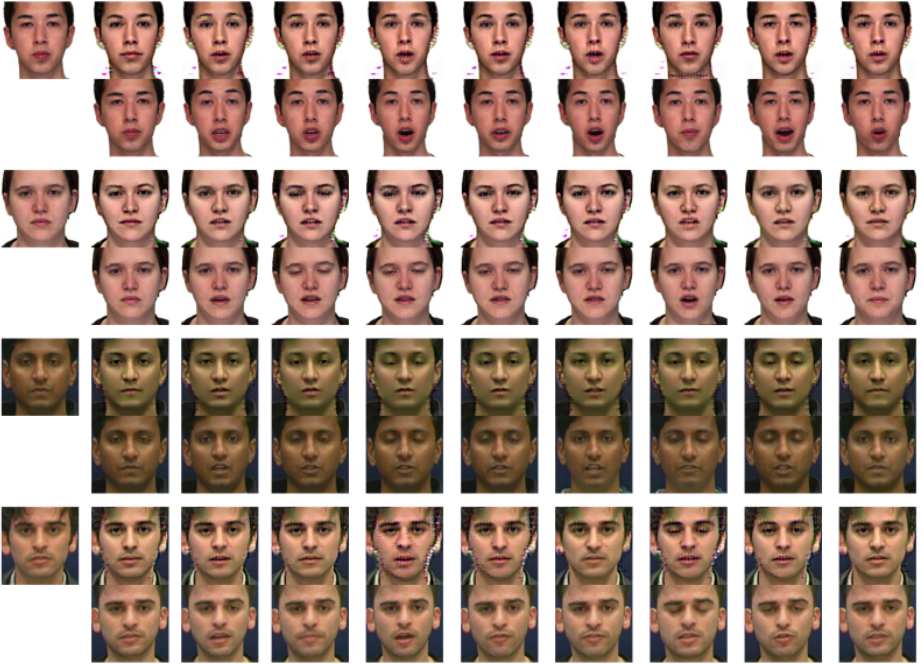


Fig. 5: Samples from four sequences in paired evaluation. For each sequence, the top left is the still source image x_{src} , and it is post-processed. x_{src} is at neutral expression. In each vertical pair, the top image is the hallucinated frame x_{tgt} , while the corresponding target frame y_{tgt} is at the bottom. In the 4th sequence, the source image and the target video were captured at two different occasions.

Table 3: RMSE of Action Unit intensity in inter-class synthesis.

GATH-DC	GATH-C	GATH
0.587	0.583	0.579

5.3 Qualitative Assessments

Figure 7 and 8 show animated sequences by GATH, in which the source images are sampled from the CelebA and LFW datasets, respectively, with diversity across genders, skin colors, styles etc. Interestingly in Figure 7c, the model even synthesizes eyes beyond the shades. More samples are shown in the supplementary video⁴.

5.4 Template-and-target-free Expression Editing

In this experiment, we perform expression suppression, transforming a face with arbitrary expression back to the neutral pose. Source images are sampled from the CelebA

⁴ <https://www.youtube.com/watch?v=Zr9M1AazPpo>



Fig. 6: Samples from three sequences, starting with non-neutral expression source images. The model learned to synthesize the "closed lip" expression when target is neutral.



Fig. 7: Samples from six animated sequences, with the source images taken randomly from CelebA dataset, with different genders, skin colors, hair styles, etc.

dataset. The qualitative results are illustrated in Figure 9,10. We transform the source to neutral expression simply by providing GATH with a zero AU vector. It proves that via our learning framework, the generator has learned to disentangle the identity code from expression. Thus, giving GATH zero AU coefficients equals generating a neutral face of the source actor.

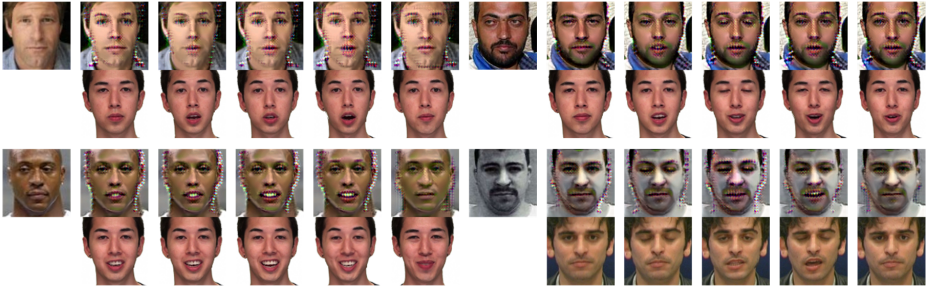


Fig. 8: Samples from four animated sequences, in which the source images were taken randomly from LFW dataset.



Fig. 9: Samples from expression suppression editing with our model on the CelebA dataset. In each pair of images, the source is on the left, the suppressed synthesis is shown on the right.

5.5 Limitations

Our GATH model has proved to be able to synthesize novel face from arbitrary source. However, there still exists some issues remaining:

- The synthesized image loses its texture dynamic range.
- There is still color noise and distortions in the reconstructed face, especially around the face contour and strong edges.

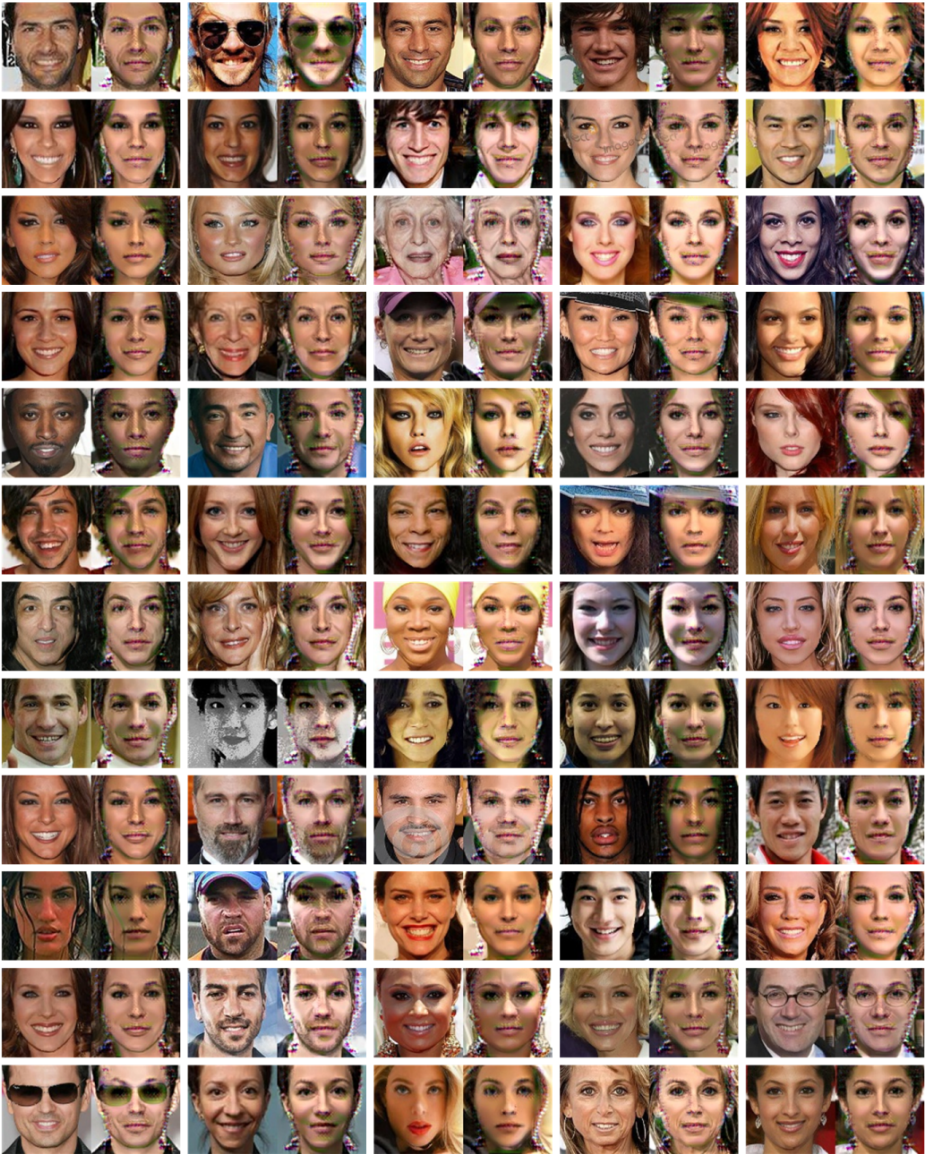


Fig. 10: More samples from expression suppression editing with our model on the CelebA dataset.

We will investigate these issues thoroughly to make GATH more robust and generate higher quality face synthesis in future work.

6 Conclusions

In this paper, we introduce Generative Adversarial Talking Head, a generative neural net that is capable of synthesizing novel faces from any source portrait given a vector of action unit coefficients. In our GATH framework, we jointly train a generator with an adversarial discriminator and a classifier, while being supervised by an AU estimator to make the generator learn correct expression deformations, as well as disentangle the identity features from expression. Our model directly manipulates image pixels to hallucinate a novel facial expression, while preserving the individual characteristics of the source face, without using a statistical face template or any texture rendering.

References

1. Averbuch-Elor, H., Cohen-Or, D., Kopf, J., Cohen, M.F.: Bringing portraits to life. *ACM Transactions on Graphics (TOG) - Proceedings of ACM SIGGRAPH Asia* **36**(196) (2017)
2. Thies, J., Zollhofer, M., Stamminger, M., Theobalt, C., Niener, M.: Face2face: Real-time face capture and reenactment of rgb videos. In: *IEEE Conference on Computer Vision and Pattern Recognition (CVPR)*. (2016)
3. Dale, K., Sunkavalli, K., Johnson, M.K., Vlasic, D., Matusik, W., Pfister, H.: Video face replacement. *ACM Transactions on Graphics (TOG)* **30**(6) (2011)
4. Garrido, P., Valgaerts, L., Rehmsen, O., Thormahlen, T., Perez, P., Theobalt, C.: Automatic face reenactment. In: *IEEE Conference on Computer Vision and Pattern Recognition*. (2014)
5. Olszewski, K., Li, Z., Yang, C., Zhou, Y., Yu, R., Huang, Z., Xiang, S., Saito, S., Kohli, P., Li, H.: Realistic dynamic facial textures from a single image using gans. (2017)
6. Cao, C., Wu, H., Weng, Y., Shao, T., Zhou, K.: Real-time facial animation with image-based dynamic avatars. *ACM Transactions on Graphics (TOG)* **35**(4) (2016)
7. Yeh, R.A., Liu, Z., Goldman, D.B., Agarwala, A.: Semantic facial expression editing using autoencoded flow. *arXiv preprint arXiv:1611.09961* (2016)
8. Pham, H.X., Cheung, S., Pavlovic, V.: Speech-driven 3d facial animation with implicit emotional awareness: a deep learning approach. In: *The 1st DALCOM workshop, CVPR*. (2017)
9. Pham, H.X., Wang, Y., Pavlovic, V.: End-to-end learning for 3d facial animation from raw waveforms of speech. *arXiv* (2017)
10. Fan, B., Xie, L., Yang, S., Wang, L., Soong, F.K.: A deep bidirectional lstm approach for video-realistic talking head. *Multimed Tools Appl* **75** (2016) 5287–5309
11. Ekman, P., Friesen, W.: Facial action coding system: A technique for the measurement of facial movement. *Consulting Psychologists Press* (1978)
12. Livingstone, S.R., Peck, K., Russo, F.A.: Ravdess: The ryerson audio-visual database of emotional speech and song. In: *22nd Annual Meeting of the Canadian Society for Brain, Behaviour and Cognitive Science (CSBBCS)*. (2012)
13. Goodfellow, I.J., Pouget-Abadie, J., Mirza, M., Xu, B., Warde-Farley, D., Ozair, S., Courville, A., Bengio, Y.: Generative adversarial nets. In: *NIPS*. (2014)
14. Radford, A., Metz, L., Chintala, S.: Unsupervised representation learning with deep convolutional generative adversarial networks. In: *International Conference on Learning Representation*. (2016)
15. Xie, L., Liu, Z.: Realistic mouth-synching for speech-driven talking face using articulatory modeling. *IEEE Trans Multimed* **9**(23) (2007) 500–510
16. Sako, S., Tokuda, K., Masuko, T., Kobayashi, T., Kitamura, T.: Hmm-based text-to-audio-visual speech synthesis. In: *ICSLP*. (2000) 25–28

17. Karras, T., Aila, T., Laine, S., Herva, A., Lehtinen, J.: Audio-driven facial animation by joint end-to-end learning of pose and emotion. In: SIGGRAPH. (2017)
18. Suwajanakorn, S., Seitz, S.M., Kemelmacher-Schlizerman, I.: Synthesizing obama: learning lip sync from audio. In: SIGGRAPH. (2017)
19. Taylor, S., Kim, T., Yue, Y., Mahler, M., Krahe, J., Rodriguez, A.G., Hodgins, J., Matthews, I.: A deep learning approach for generalized speech animation. In: SIGGRAPH. (2017)
20. Qian, Y., Fan, Y., Soong, F.K.: On the training aspects of deep neural network (dnn) for parametric tts synthesis. In: ICASSP. (2014) 3829–3833
21. Zen, H., Senior, A., Schuster, M.: Statistical parametric speech synthesis using deep neural networks. In: ICASSP. (2013) 7962–7966
22. Ding, C., Xie, L., Zhu, P.: Head motion synthesis from speech using deep neural network. *Multimed Tools Appl* **74** (2015) 9871–9888
23. Zhang, X., Wang, L., Li, G., Seide, F., Soong, F.K.: A new language independent, photo realistic talking head driven by voice only. In: Interspeech. (2013)
24. Denton, E., Chintala, S., Szlam, A., Fergus, R.: Deep generative image models using a laplacian pyramid of adversarial networks. In: NIPS. (2015)
25. Ledig, C., Theis, L., Huszar, F., Caballero, J., Cunningham, A., Acosta, A., Aitken, A., Tejani, A., Totz, J., Wang, Z., Shi, W.: Photo-realistic single image super-resolution using a generative adversarial network. In: IEEE International Conference on Computer Vision and Pattern Recognition. (2017)
26. Reed, S., Akata, Z., Yan, X., Logeswaran, L., Lee, H., Schiele, B.: Generative adversarial text to image synthesis. In: International Conference on Machine Learning. (2016)
27. Isola, P., Zhu, J.Y., Zhou, T., Efros, A.A.: Image-to-image translation with conditional adversarial networks. In: IEEE International Conference on Computer Vision and Pattern Recognition. (2017)
28. Choi, Y., Choi, M., Kim, M., Ha, J.W., Kim, S., Choo, J.: Stargan: Unified generative adversarial networks for multi-domain image-to-image translation. *arXiv* (2017)
29. Mirza, M., Osindero, S.: Conditional generative adversarial nets. *arXiv* (2014)
30. Springenberg, J.T.: Unsupervised and semi-supervised learning with categorical generative adversarial networks. In: International Conference on Learning Representation. (2016)
31. Odena, A., Olah, C., Shlens, J.: Conditional image synthesis with auxiliary classifier gans. In: International Conference on Machine Learning. (2017)
32. Tran, L., Yin, X., Liu, X.: Disentangled representation learning gan for pose-invariant face recognition. In: IEEE International Conference on Computer Vision and Pattern Recognition. (2017)
33. Li, C., Xu, K., Zhu, J., Zhang, B.: Triple generative adversarial nets. In: 31st Conference on Neural Information Processing Systems (NIPS). (2017)
34. Blanz, V., Vetter, T.: A morphable model for the synthesis of 3d faces. In: SIGGRAPH. (1999) 187–194
35. Vlastic, D., Brand, M., Pfster, H., Popovi, J.: Face transfer with multilinear models. *ACM Transactions on Graphics (TOG)* **24** (2005)
36. Blanz, V., Basso, C., Poggio, T., Vetter, T.: Reanimating faces in images and video. In: Eurographics. (2003) 641–650
37. Yang, F., Wang, J., Shechtman, E., Bourdev, L., Metaxas, D.: Expression ow for 3d-aware face component transfer. *ACM Transactions on Graphics (TOG)* **30** (2011)
38. Yang, F., Bourdev, L., Shechtman, E., Wang, J., Metaxas, D.: Facial expression editing in video using a temporally-smooth factorization. In: IEEE Conference on Computer Vision and Pattern Recognition (CVPR). (2012)
39. Liu, Z., Shan, Y., Zhang, Z.: Expressive expression mapping with ratio images. In: Proceedings of the 28th annual conference on Computer graphics and interactive techniques. (2001)

40. Liu, Z., Song, G., Cai, J., Cham, T.J., Zhang, J.: Conditional adversarial synthesis of 3d facial action units. arXiv (2017)
41. Kingma, D.P., Welling, M.: Auto-encoding variational bayes. In: ICLR. (2014)
42. : Deepfakes. <https://github.com/deepfakes/faceswap>
43. Kulkarni, T.D., Whitney, W., Kohli, P., Tenenbaum, J.B.: Deep convolutional inverse graphics network. In: NIPS. (2015)
44. Yang, J., Reed, S., Yang, M.H., Lee, H.: Weakly-supervised disentangling with recurrent transformations for 3d view synthesis. In: NIPS. (2015)
45. Peng, X., Feris, R.S., Wang, X., Metaxas, D.: A recurrent encoder-decoder network for sequential face alignment. In: ECCV. (2016)
46. Cao, C., Weng, Y., Zhou, S., Tong, Y., Zhou, K.: FaceWarehouse: A 3D Facial Expression Database for Visual Computing. *IEEE Transactions on Visualization and Computer Graphics* **20**(3) (March 2014) 413–425
47. Gatys, L.A., Ecker, A.S., Bethge, M.: A neural algorithm of artistic style. *CoRR abs/1508.06576* (2015)
48. Simonyan, K., Zisserman, A.: Very deep convolutional networks for large-scale image recognition. *CoRR abs/1409.1556* (2014)
49. Zhu, J.Y., Park, T., Isola, P., Efros, A.A.: Unpaired image-to-image translation using cycle-consistent adversarial networks. In: *IEEE International Conference on Computer Vision (ICCV)*. (2017)
50. He, K., Zhang, X., Ren, S., Sun, J.: Deep residual learning for image recognition. In: *CVPR*. (2016)
51. Chen, B.C., Chen, C.S., Hsu, W.H.: Face recognition and retrieval using cross-age reference coding with cross-age celebrity dataset. *IEEE Transactions on Multimedia* **17**(6) (2015) 804–815
52. Tarrs, F., Rama, A.: GTAV face database. <https://gtav.upc.edu/research-areas/face-database>
53. Sanderson, C., Lovell, B.: Multi-region probabilistic histograms for robust and scalable identity inference. *Lecture Notes in Computer Science (LNCS)* **5558** (2009) 199–208
54. Pham, H.X., Pavlovic, V., Cai, J., jen Cham, T.: Robust real-time performance-driven 3d face tracking. In: *ICPR*. (2016)
55. Pham, H.X., Pavlovic, V.: Robust real-time 3d face tracking from rgbd videos under extreme pose, depth, and expression variations. In: *3DV*. (2016)
56. Hassner, T., Harel, S., Paz, E., Enbar, R.: Effective face frontalization in unconstrained images. In: *IEEE International Conference on Computer Vision and Pattern Recognition*. (2015)
57. Kingma, D.P., Ba, J.: Adam: A method for stochastic optimization. In: *3rd International Conference for Learning Representations*. (2015)
58. Zuiderveld, K.: Contrast limited adaptive histogram equalization. *Graphic Gems IV* (1994) 474–485
59. Buades, A., Coll, B., Morel, J.M.: Non-Local Means Denoising. *Image Processing On Line* **1** (2011) 208–212
60. Baltruaitis, T., Robinson, P., , Morency, L.P.: Openface: an open source facial behavior analysis toolkit. In: *IEEE Winter Conference on Applications of Computer Vision*. (2016)
61. Liu, Z., Luo, P., Wang, X., Tang, X.: Deep learning face attributes in the wild. In: *Proceedings of International Conference on Computer Vision (ICCV)*. (2015)
62. Huang, G.B., Ramesh, M., Berg, T., Learned-Miller, E.: Labeled faces in the wild: A database for studying face recognition in unconstrained environments. Technical Report 07-49, University of Massachusetts, Amherst (October 2007)